Journal of Experimental Biology and Agricultural Sciences, February - 2022; Volume – 10(1-BIONEXT-2021) page 254 – 265

Journal of Experimental Biology and Agricultural Sciences

http://www.jebas.org

ISSN No. 2320 – 8694

Biosorption of Acid dye by Jackfruit Leaf Powder: Isotherm, kinetics and Response surface methodology studies

Swagata Roy Chowdhury[1], Sebak Ranjan Roy[2], Aritra Ganguly[3], Rounak Ghosh[3], Suvajit Majumder[3], Archita Dasgupta[3], Ranjan Das[3], Anupam Kumar[3], Animesh Naskar[2*], Rajib Majumder[1*]

[1]Department of Biotechnology, School of Life Science & Biotechnology, ADAMAS University, Kolkata, India
[2]Department of Food Science and Technology, Maulana Abul Kalam Azad University of Technology, Haringhata, West Bengal-741249, India
[3]Department of Food Technology, Hemnalini Memorial College of Engineering, Maulana Abul Kalam Azad University of Technology, West Bengal -741246, India

Received – October 16, 2021; Revision – November 24, 2021; Accepted – December 09, 2021
Available Online – February 28, 2022

DOI: http://dx.doi.org/10.18006/2022.10(1).254.265

KEYWORDS

Biosorption

Acid dye

Jackfruit leaf

Response surface methodology

Kinetics

ABSTRACT

A green adsorbent derived from Jackfruit leaf powder (JLP) was used to eliminate Acid Yellow 99 (AY 99) dye from an aqueous medium in this study. We checked the effect of pH, biomass dosage, and temperature (process parameters) on the adsorption potential of AY 99 was explored using the CCD model integrating the RSM approach. At a pH of 2.5, biosorbent dosage of 4 gL^{-1}, and a 30°C temperature, maximum removal was preferred. ANOVA was incorporated to observe the importance of experimental variables and their interactions. The solution pH (A) and biomass dose (C) had the greatest effects on the decolorization of AY 99, according to the findings. ANOVA was used to identify the most important factors, which included two independent variables (A and C) and two quadratic model terms (A^2 and C^2). The kinetic data were effectively interpreted using a pseudo 2^{nd} order with film diffusion model combination, indicating the chemisorptions phenomenon. Following the model of Langmuir isotherm, the utmost capacity for adsorption was determined to be 418.15 mg g^{-1} in terms of initial dye concentration. The findings of the maximum adsorption capacity showed that JLP could be employed as a useful adsorbent to eliminate AY 99 from its aqueous medium.

* Corresponding author

E-mail: rajib.iicb@gmail.com (Dr. Rajib Majumder);
animesh.ftbe@gmail.com (Dr. Animesh Naskar)

Peer review under responsibility of Journal of Experimental Biology and Agricultural Sciences.

Production and Hosting by Horizon Publisher India [HPI] (http://www.horizonpublisherindia.in/).

1 Introduction

Water is an essential ecological resource for the survival of all living things on the planet. Pollution of water is a foremost worry in today's world (Wang et al. 2021). Acid Yellow 99, a negatively charged azo dye, is not biodegradable due to its complex organic structure (Khan et al. 2019). A large volume of dye is produced and used for mankind's benefit through various industrial processes, and wastewater contain an alarming amount of dye and harmful auxiliary compounds, all of which contribute to chemical oxygen demand (De Castro et al. 2018). The presence of these xenobiotic chemicals in natural water bodies has negative consequences for both the ecosystem and living creatures. Due to the limited penetration of sunlight, dye slows the growth of phototrophs and autotrophs in water (Lellis et al. 2019). As a result, dye-bearing wastewater must be treated before being discharged onto the earth's surface, as required by the BIS directive (Khan et al. 2019). However, many industries are still grappling with how to properly dispose of these wastes. Bio-adsorption has recently gained prominence in this area, owing to its superior benefits over traditional physicochemical procedures for dealing with dye effluents in an aqueous solution (Putri et al. 2021). Although bio-adsorption is most commonly utilized for metal binding, it can also be used to remove hazardous dyes as a cost-effective and alternative method for treating industrial wastewater and contributing to environmental remediation. The degree to which a pollutant is removed is determined by equilibrium and kinetics, both of which are influenced by experimental conditions. As a result, determining the bio-adsorption of a contaminant by biomass is an intricate task (Priyantha et al. 2018). The method primarily imports low-cost bio-based substances such as plant derivatives, microbial cells, and other bio-based substances with simple instrumental procedures at a low cost (Gupta et al. 2019). According to the survey, tons of agricultural wastes have been generated each year globally (Duque-Acevedo et al. 2020). The use of these low-cost, renewable wastes for water purification appears to be a significant step towards long-term sustainability.

The leaves of the jackfruit (*Artocarpus heterophyllus*) are attractive biosorbent materials that are low-cost and widely available in India and other areas of the world. This agricultural waste is made up of a variety of biomolecules, including proteins, lipids, and carbohydrates, all of which have active functional groups that are thought to be larger entities for dye interactions. (Das and Mishra 2019). The efficacy of biosorbents, on the other hand, is dependent not only on their physicochemical properties but also on the microenvironment of the target pollutant. Only a few studies have shown that raw Jackfruit leaf powder can be used to remove methylene blue (Uddin et al. 2009), crystal violet (Saha et al. 2012), Amido black 10B (Ojha and Bulasara 2015), and nickel (Ranasinghe et al. 2018). However, these techniques are still under development. There has been no research into the removal of Acid yellow 99 dye using such biosorbent (JLP) in its natural form to the best of our knowledge.

Despite these promising advantages, the design of the experiment (DOE) using RSM has been used to construct the most reliable batch adsorption system. The approach is especially well adapted to optimizing experimental findings, evaluating the effect of variables, and evaluating their interaction with a collection of least experiments (Bagheri et al. 2019; Naskar et al. 2020).

Considering the above background, the main objectives of this research are (1) to evaluate its potential for removing Acid Yellow 99 (AY 99) from the aqueous medium, (2) to investigate the process controlling parameters through RSM modelling in order to achieve the optimum ones with simultaneous variable interactions, and (3) to gain a better understanding of mechanisms during dye-biomass interactions.

2 Material and Methods

2.1 Reagents and chemicals

The Acid-Yellow (AY) 99 dye (C.I. 13900) was procured from Sigma-Aldrich, U.S. Other necessary chemicals required for completing the experiments were supplied by E-Merck, Germany.

2.2 Estimation and calibration of AY-99 dye solution

A UV-vis spectrophotometer (Perkin Elmer λ-25, Singapore) was used to calculate the dye concentration considering the calibration curve created from dye standards. The mass balance equation can be used to estimate the quantity of dye absorbed by the JLP biomass (mg g^{-1}) (Eq. 1) (Khan et al. 2011):

$$q_e = \frac{(C_0 - C_e)V}{1000W} \quad (1)$$

Here q_e depicts dye uptake (mg g^{-1}), C_0 denotes initial dye conc. (mg L^{-1}), and C_e highlights the dye conc. at equilibrium (mg L^{-1}), V indicates the working dye volume (in mL) and W is biomass weight used in each experiment (g)

2.3 Biosorbent: Jackfruit Leaf Powder (JLP)preparation

Jackfruit (*Artocarpus heterophyllus*) leaves were picked locally and washed well with tap water. Later on, these were further washed by double distilled water to eliminate redundant adhering dirt materials. The washed leaves were oven-dried at 70±5°C overnight to obtain the fine powder through the mechanical grinder.

2.4 Biosorption experiments through RSM modelling

RSM, a statistical technique was employed to examine the influence of essential physicochemical factors and to establish the optimum amount of variables for maximum dye decontamination by JLP. The three factors, along with their coded and real forms, were designed at three separate levels with the help of Design Expert (DE) version 12 (Stat-Ease, Inc., USA), as shown in Table 1. The influence of three independent variables affecting dye removals, such as starting pH (A), temperature (B), and biomass dose (C), was investigated using statistical models in this study. Various combinations of Six (6) axial points, Eight (8) factorial points, and Six (6) centre points were used in a set of 20 experimental runs (Table 2). The dye absorption (mg g^{-1}) was regarded as a system's dependent output response (Y). The quadratic model equation that was utilized to derive expected responses was (Eq. 2):

$$Y = \beta_o + \sum \beta_i x_i + \sum \beta_{ij} x_i x_j + \sum \beta_{ii} x_i^2 \quad (2)$$

Here Y denotes predicted responses, β_o denotes the offset term, β_i and β_{ii} reflects the linear outcome and squared effect respectively. β_{ij} represent the interaction effect, x_i denotes ith independent variable, $x_i x_j$ indicates interaction term and x_i^2 highlights the quadratic terms.

The F-value and R^2 (regression coefficient) was used to evaluate the model's fittest and accuracy. This software was used to solve the regression equations, the three-dimensional (3D) responses for the different parameters to find the best conditions for dye uptake by the JLP.

Table 1 Experimental ranges with three different levels in the experimental design

Factor	Name	Units	Minimum	Maximum	Coded Low	Coded High	Mean
A	pH		2.00	3.00	-1 ↔ 2.00	+1 ↔ 3.00	2.50
B	Temperature	℃	20.00	40.00	-1 ↔ 20.00	+1 ↔ 40.00	30.00
C	Biomass dose	g L^{-1}	3.00	5.00	-1 ↔ 3.00	+1 ↔ 5.00	4.00

Table 2 CCD Design with the actual and predicted response

Run Order	Factor-A pH	Factor-B Temp (℃)	Factor-C Biomass dose (g/L)	Space Type	Actual Response (mg/g)	Predicted Response (mg/g)
1	3	40	5	Factorial	21.10	21.06
2	2.5	30	3	Axial	20.41	20.91
3	2.5	30	4	Center	23.69	23.56
4	2.5	40	4	Axial	23.81	23.99
5	3	30	4	Axial	19.34	19.83
6	2.5	30	4	Center	23.67	23.56
7	2	30	4	Axial	21.29	21.20
8	2.5	30	4	Center	23.70	23.56
9	2.5	30	5	Axial	24.01	23.92
10	3	40	3	Factorial	17.59	17.39
11	2	40	5	Factorial	21.75	21.84
12	2.5	30	4	Center	23.65	23.56
13	2	20	5	Factorial	21.43	21.53
14	2.5	30	4	Center	23.75	23.56
15	2.5	20	4	Axial	23.52	23.74
16	3	20	3	Factorial	17.40	17.21
17	2	40	3	Factorial	18.97	18.93
18	3	20	5	Factorial	20.38	20.32
19	2	20	3	Factorial	19.23	19.17
20	2.5	30	4	Center	23.71	23.56

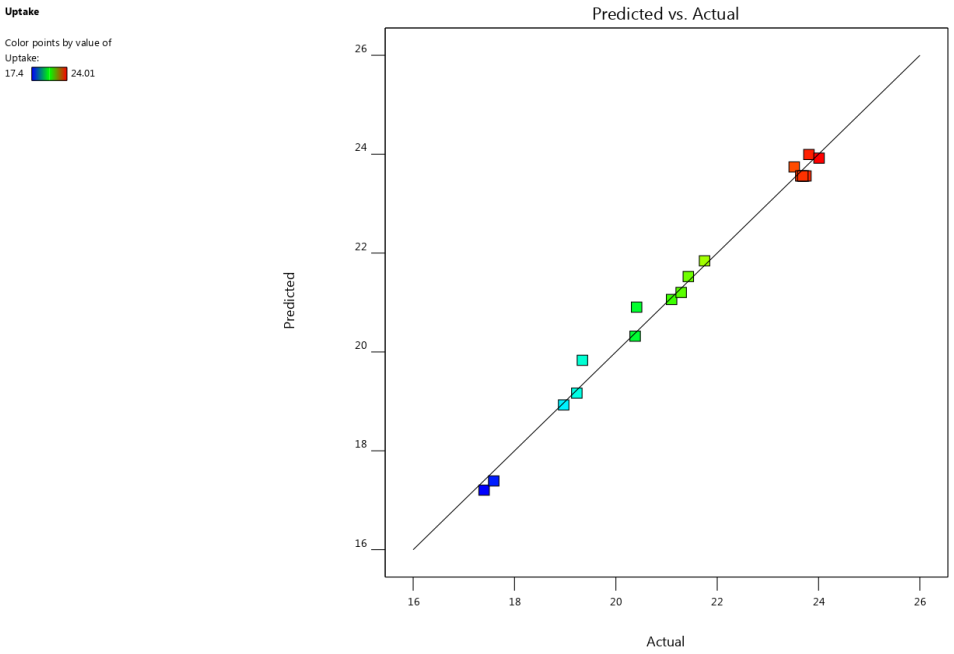

Figure 1 Actual versus predicted graph for adsorption of AY-99 by JLP biomass

2.5 Dye biosorption experiment

All biosorption experiments for decontaminating AY-99 by JLP were carried out in Erlenmeyer flasks (250 mL) with a 50 mL dye test solution of 100 mg L^{-1} at pH 2.5. The flasks were agitated well (120 rpm) in a temperature-controlled shaker incubator. After that, the biomass was removed from the solution using Millipore membrane vacuum filtrations, and the residual dye concentration was quantified using a UV-visible spectrophotometer.

For isotherm studies, the desired quantity of JLP was exposed to 50 mL of dye (concentrations ranging 50–5000 mg L^{-1}) of pH 2.5 at 30°C. Moreover, dye removal with respect to contact time was examined in Erlenmeyer flasks containing dye solution (100 mg L^{-1}) pH 2.5 with a fixed biomass dose of 4 g L^{-1}.

2.6 Statistical analysis

Using Design-Expert 12.0.0.6, each of the experiments was carried out for three times and the mean results were given in the result and discussion section, taking into account the p-value (0.05). The Origin 8.0 programme calculated the Chi-square analytical result and the experiment regression coefficient.

3 Results and Discussion

3.1 Central composite design and statistical evaluation

The experimental run is depicted in Table 2 along with a summary of the outcomes. The pragmatic association between independent factors and intended responses was discovered and stated by the following SOPE, according to the findings:

$$\text{Uptake} = +23.56 - 0.6860A + 0.1260B + 1.51C + 0.1063AB + 0.1887AC + 0.1388BC - 3.04A^2 + 0.3086B^2 - 1.15C^2$$

Where A, B, and C correspond to independent variables of pH, temperature (ºC), and biomass dose (g L^{-1}), respectively. Uptake is the response (Y) here. The equation with coded factors, on the other hand, may be used to predict response for different amounts of individual factors. In general, the factors' upper levels are recorded as +1, while -1 codes the lower levels of the factor. The coding equation can be used to calculate the relative significance of the factors compared with the coefficients of the factors. The coefficient provides the estimated change (response/unit change) in values of the factor while all other factors are kept constant. For orthogonal design, the intercept is the total average response in all runs. Experimental coefficients were adjustments, which depend on factor settings in the vicinity of the average. When the factors were orthogonal, the VIFs are 1; VIFs more than 1 denote multicollinearity, and higher this VIF reflects more extreme factor correlation. VIFs of less than ten are regarded as acceptable. The F-value of 129.88 for the model suggests that it is statistically significant. Due to noise, an F-value of this magnitude has a 0.01 percent probability of occurring. P-values < 0.0500 indicated that all model terms were significant. In the present scenario, two independent factors (A and C), as well as two quadratic model terms (A^2 and C^2), were found to be significant in affecting dye uptake (Table 3). If the value is more than 0.1000, the model terms

are irrelevant. The Adjusted R^2 of 0.9839 is reasonably fit to the Predicted R^2 of 0.9487. There only the difference is < 0.2. Alongside, the signal-to-noise ratio was calculated with sufficient precision. It is recommended to have a higher ratio than 4. In this experiment, the signal-to-noise ratio of 33.755 indicates that the signal is satisfactory. Accordingly, this model can be applied to the design process. Additional statistical parameters [mean (21.62), standard deviation (0.2844), and the coefficient of variance (1.32 %)] summarised in Table 4 also indicated the significance of our tested model. Moreover, with a high regression coefficient, the experimental outcomes were highly correlated to predicted responses, underlying the appropriate analysis for the datasets.

3.2 Biosorption of dye depends on pH and biomass dose: Response surface plots

We have chosen several key independent parameters in this investigation [A: pH, B: temperature (^oC), C: biomass dose (g L^{-1})]. The solution pH and the biomass dose had a substantial impact on the results. The surface charge of the biosorbent and the adsorbate behavior are both influenced by the pH of the solution in the dye adsorption process. At pH 2.5, the greatest adsorption capacity (24.01 mg g^{-1}) was recorded, and as the pH was increased, the adsorption capacity decreased. At pH 2.5, dye occurs as negatively charged species and is adsorbed on positively charged entities utilizing elevated electrostatic attraction, resulting in improved adsorption potential (Naskar and Majumder 2017). Increases in pH values from 2.5 to 6.0 resulted in proportional decreases in dye absorption capacity, as shown in Figure 2. The biomass surface becomes negative in charge as the pH rises (pH > 2.5), reducing dye interaction because of electrostatic repulsion. Our findings are also in line with those of other studies (Khan et al. 2011;

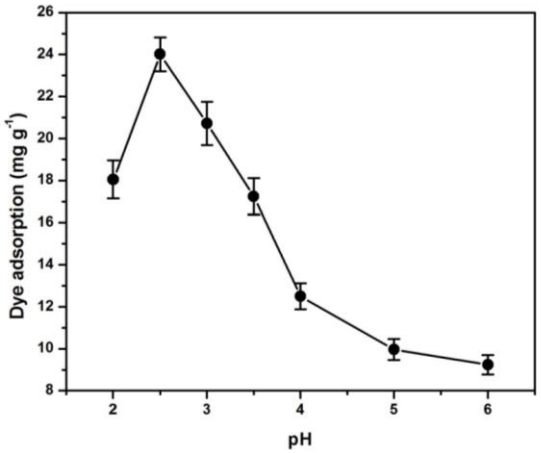

Figure 2 Effect of solution pH on AY-99 adsorption by JLP biomass (temperature: 30ºC, speed of agitation: 120 rpm and dye concentration: 100 mg L^{-1}): ±SD shown with error bars.

Table 3 ANOVA analysis regarding to AY 99 adsorption by JLP

Source	Sum of Squares	df	Mean Square	F-value	p-value	
Model	94.57	9	10.51	129.88	< 0.0001	significant
A-pH	4.71	1	4.71	58.17	< 0.0001	
B-Temp	0.1588	1	0.1588	1.96	0.1915	
C-dose	22.71	1	22.71	280.72	< 0.0001	
AB	0.0903	1	0.0903	1.12	0.3156	
AC	0.2850	1	0.2850	3.52	0.0900	
BC	0.1540	1	0.1540	1.90	0.1977	
A^2	25.44	1	25.44	314.42	< 0.0001	
B^2	0.2620	1	0.2620	3.24	0.1021	
C^2	3.61	1	3.61	44.67	< 0.0001	
Residual	0.8090	10	0.0809			
Lack of Fit	0.8031	5	0.1606	134.97	< 0.0001	significant
Pure Error	0.0060	5	0.0012			
Core Total	95.37	19				

Table 4 Fit Statisticsregarding to AY 99 adsorption by JLP

Std. Dev.	0.2844	R^2	0.9915
Mean	21.62	Adjusted R^2	0.9839
C.V. %	1.32	Predicted R^2	0.9487
		Adeq Precision	33.7552

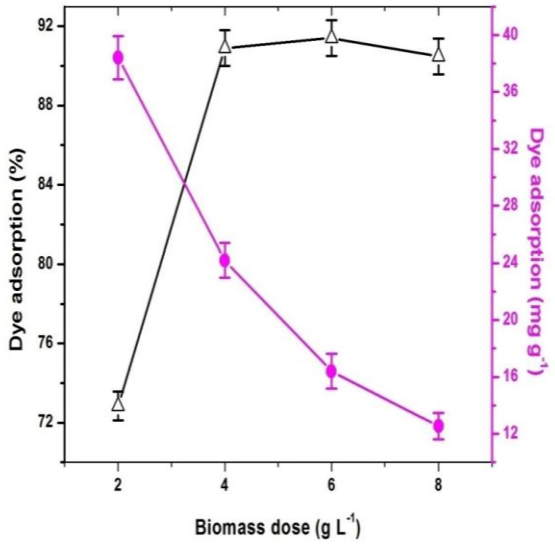

Figure 3 Influence of biomass dose on AY-99 adsorption by JLP

Khan et al. 2019). Another key aspect was investigated, and dye removal effectiveness rose progressively with increasing biomass dose, with 4 g L^{-1} biomass at pH 2.5 achieving optimum removal (~92 %). This could be owing to an increase in adsorbent particle contact surface due to increased biomass and more accessible binding sites for dye complexation (Cheruiyot et al. 2019). Further increased biomass dosage (6 g L^{-1}) has no discernible effect on dye decolourisation. Furthermore, the experimental results shown in Figure 3 reveal that the maximal dose (8 g L^{-1}) results in a little reduction (89%) in the dye removal pattern. The aggregation of active sites may explain this unequal adsorption behaviour, resulting in a modest decrease in dye removal (%). Furthermore, a larger dosage has a negative impact on biomass dye absorption capacity (mg g^{-1}). Other factors, such as temperature, had no significant impact on dye adsorption.

The perturbation graph of the 3 independent variable factors is depicted in Figure 4. According to this plot, the model's centre point, factors A (pH), exhibits a positive response at first, then a negative response moves away from that reference point. The plot clearly showed that the lower the pH, the more dye was removed, as our earlier research had demonstrated the same phenomenon (Khan et al. 2011; Naskar and Majumder 2017). The combined effects of pH-temperature (Figure 5), pH-biomass dose (Figure 6), and temperature-biomass dose (Figure 7) were demonstrated in this work using three response surface 3D plots. An elliptical 3D response surface plot regarding to pH and biomass dose demonstrated that the interactions between these factors were extremely significant, according to this finding. The following were the optimum levels of each variable in real values: pH = 2.5, temperature = 30 ºC, and biomass dose = 4 g L^{-1}, all of them fell inside the experimental series. The findings have corroborated with other research works (Khan et al. 2011; Naskar and Majumder 2017). Under these ideal conditions, the experimental response was 24.01 mg g^{-1}, which was very similar to the yield predicted by the statistical model (23.92 mg g^{-1}), with an R^2 value of 0.9915.

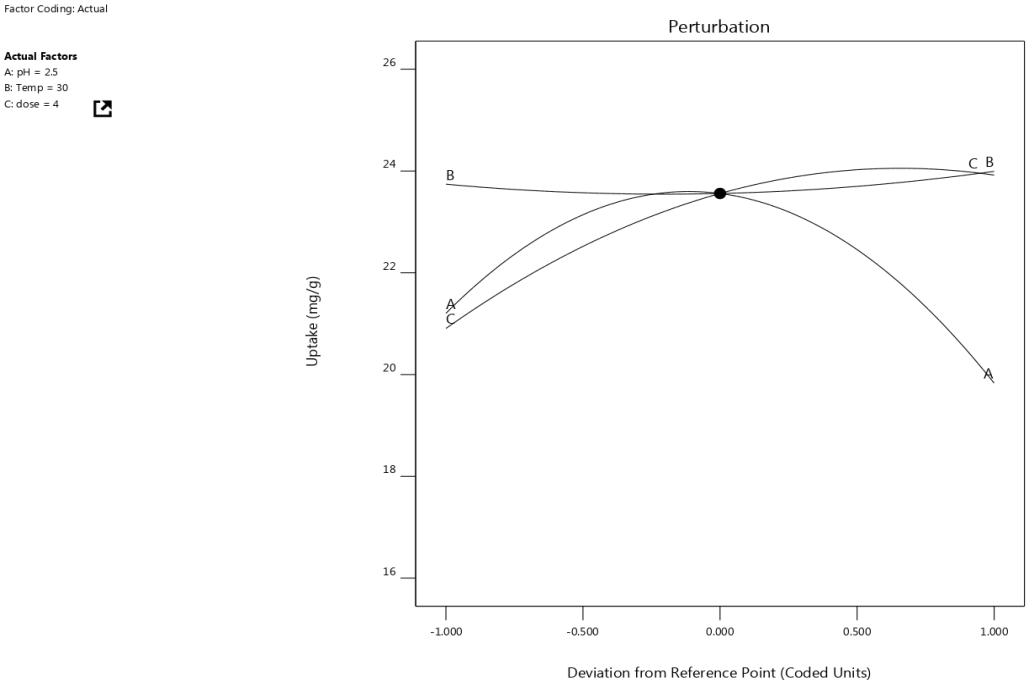

Figure 4 Perturbation plot on AY 99 adsorption by JLP biomass.

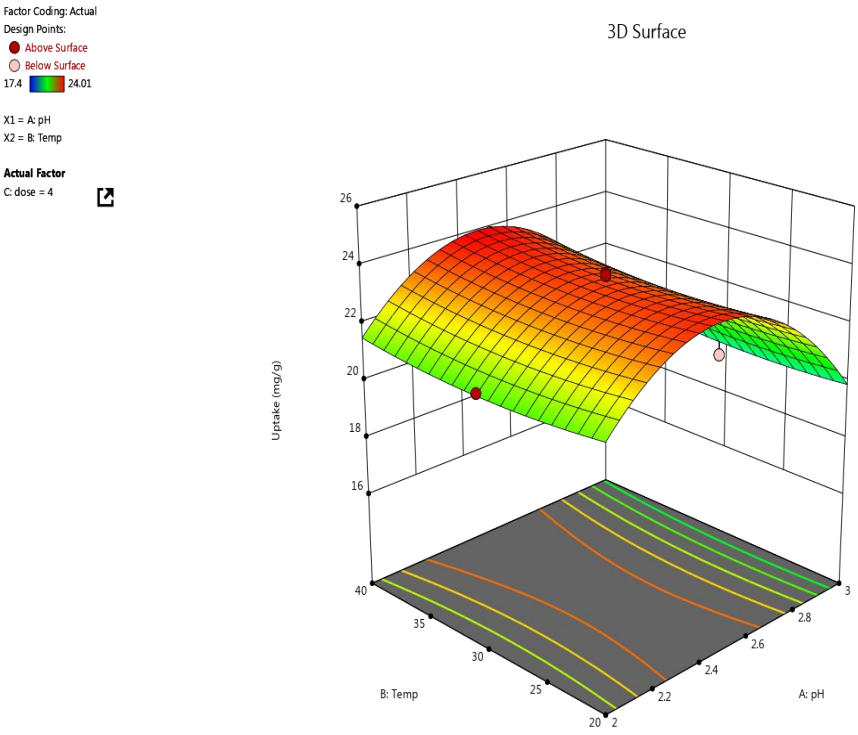

Figure 5 3Dimentional plot of pH versus temperature on AY 99 adsorption by JLP biomass.

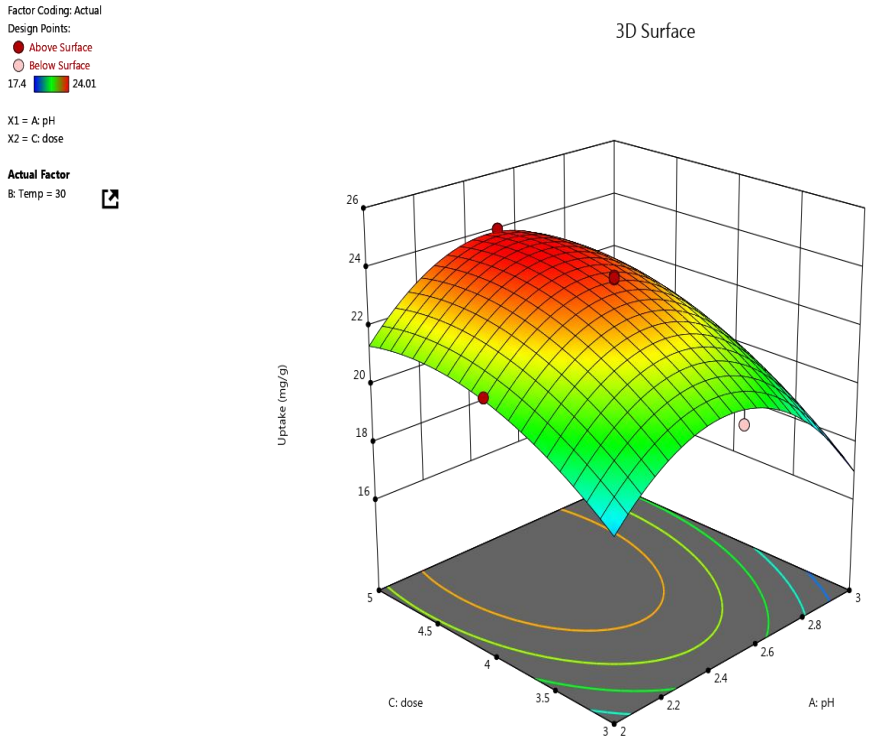

Figure 6 3D plot of pH versus biomass dose on AY 99 adsorption by JLP biomass.

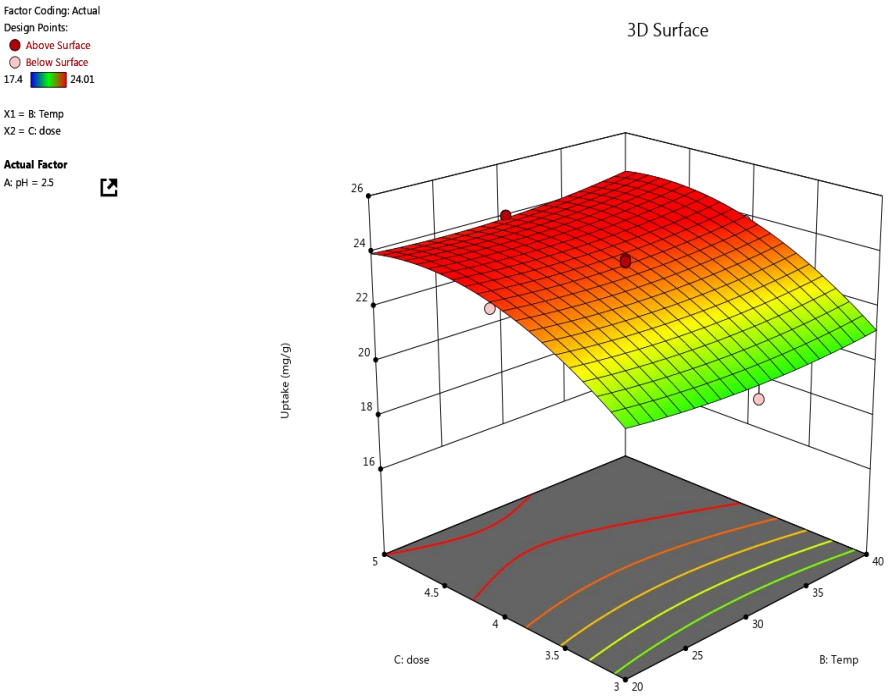

Figure 7 3D plot of biomass dose versus temperature on AY 99 adsorption by JLP biomass.

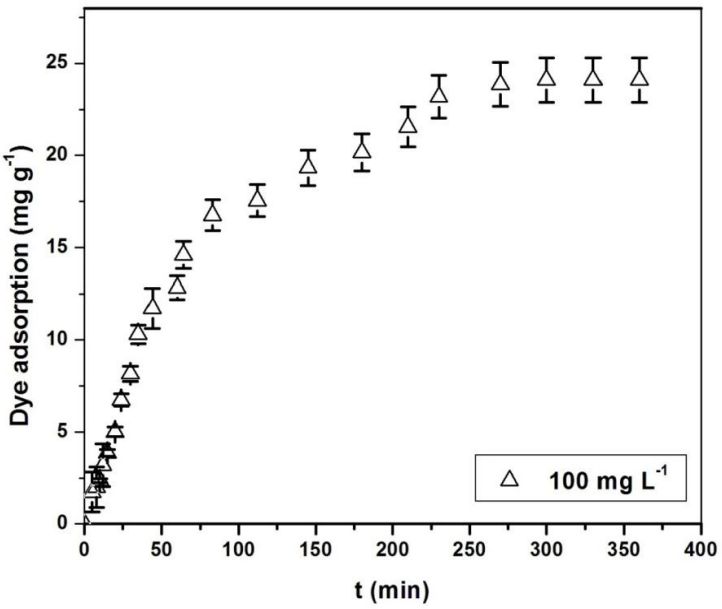

Figure 8 Influence of surface contact time on AY-99 dye adsorption by JLP biomass (b): ±SD shown with error bars.

3.3 Effect of SCT and kinetic study

The most crucial parameter is the contact time to forecast the rate of reaction and the mechanisms of dye removal by JLP (Saxena et al. 2020). The result revealed in Figure 8 speaks an initial rapid attachment of AY-99 with readily available active sites of JLP by electrostatic interaction or passive uptake by the physical force of attractions, followed by film mass transfer and finally accomplished in equilibrium state within 250 min by sluggish intra-particle diffusion (Basu et al. 2017). Similarly, Ozcan and Ozcan (2008) and Khan et al. (2011) reported this phenomenon earlier for the removal of AY-99 by DEDMA- sepiolite and coir

pith, respectively. This is noteworthy to mention that ~75% of the dye could be removed by JLP during the early 55 min thereby ensuring its prospect in the real process.

A step forward investigation was carried out by associating the experimental outcomes to widely accepted kinetic models and diffusion models to understand the mechanisms of mass transfer as well as the rate-controlling stage. The linear equation of (PFO) pseudo 1st order (Eq. 3) and (PSO) pseudo 2nd order (Eq. 4), intra-particle diffusion (IPD) (Eq. 5), and film diffusion (Eq. 6) model are as follows (Naskar and Bera 2018).

$$\ln(q_e - q_t) = \ln q_e - k_1 t \quad (3)$$

$$\frac{t}{q_t} = \frac{1}{k_2 q_e^2} + \frac{t}{q_e} \quad (4)$$

$$q_t = k_p t^{1/2} + C \quad (5)$$

$$\ln(1-F) = -K_f t \quad (6)$$

Here q_e is the dye uptake in equilibrium (in mg g^{-1}) and q_t is dye uptake at time 't'(mg g^{-1}), the rate constants of PFO (min^{-1}), PSO (mg g^{-1} min^{-1}), IPD (mg g^{-1} $min^{-1/2}$) and film diffusion, were denoted by k_1, k_2, k_p and k_f, respectively, intercept (mg g^{-1}) is highlighted by C obtained from q_t vs $t^{1/2}$ plot, and F stands for the fractional achievement of equilibrium.

Table 5 shows the calculated findings of the PSO kinetic model (Figure 9) has a higher R^2 (correlation coefficient) than the PFO model (Figure 10). Alongside, the experimental adsorption capacity (24.06 mg g^{-1}) is near to the model calculated value (26.34 mg g^{-1}) for the pseudo 2nd order kinetic model. Therefore, under the observed experimental conditions, chemisorption may be considered for the rate limiting step in the removal of AY 99 by JLP biomass (Khan et al. 2011).

Because the preceding kinetic models are unable to describe the diffusion mechanism, the intraparticle diffusion and film diffusion models are used to further explore the experiment data (Majumder et al. 2017). Table 5 shows the experimental findings for the intraparticle diffusion model. A plot of q_t vs $t^{1/2}$ revealed a triphasic nature (Figure not shown). As a result, the curve and plot were nonlinear and did not intersect the origin, showing that IPD is

Table 5 The tabulated kinetic parameters for AY 99 removal by JLP biomass

Dye (mg L^{-1})	FOK			SOK			IPD			Film diffusion	
	k_1	q_e	R^2	k_2	q_e	R^2	k_p	C	R^2	K_f	R^2
100	0.013	15.89	0.949	6.9×10^{-4}	26.34	0.984	1.143	0.097	0.892	1.1×10^{-2}	0.979

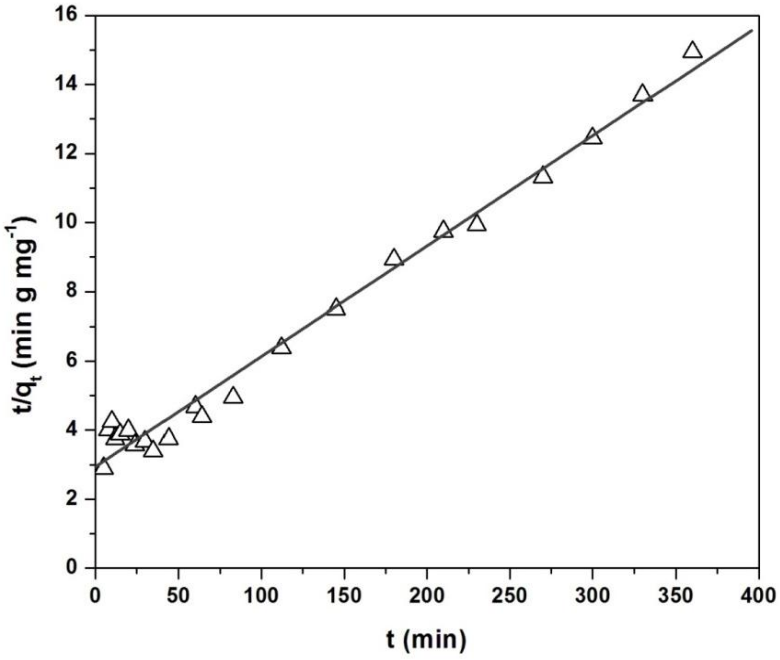

Figure 9 Plot of Pseudo 2ndorder kinetics on adsorption of AY 99 by JLP biomass.

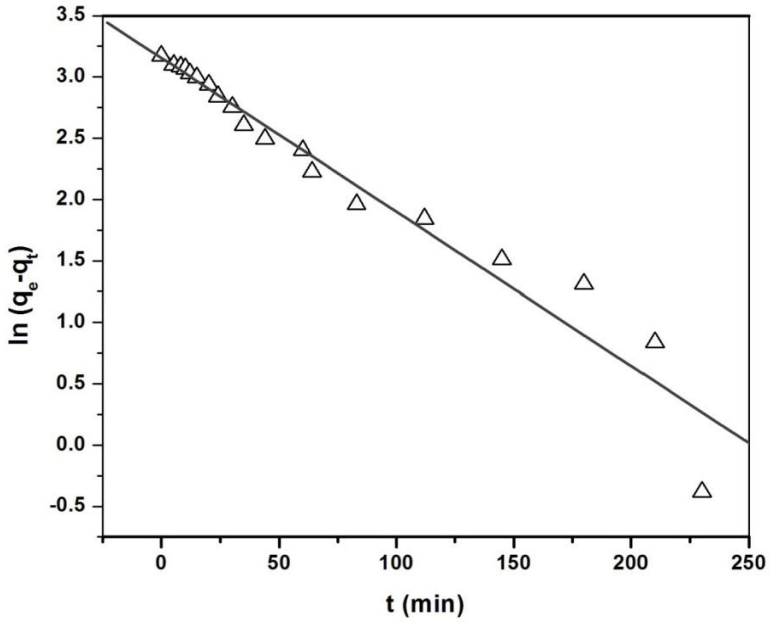

Figure 10 Pseudo-first order kinetics plot on adsorption of AY 99 by JLP biomass.

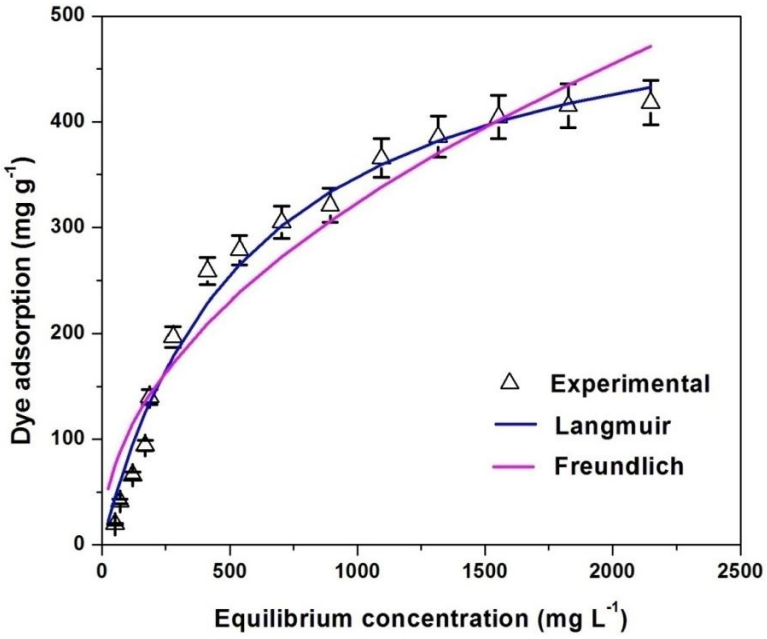

Figure 11 Adsorption isotherm of the dye (AY 99) on JLP biomass (pH: 2.5, temperature: 30ºC, and speed of agitation: 120 rpm)

significant but not only rate-determining phase in the overall dye elimination procedure. On the contrary, for the film diffusion-driven transport mechanism, the fitted straight line plots of ln (1 − F) vs.'t' revealed a high grade correlation coefficient (0.979). Furthermore, a little magnitude of intercept of 5.28×10^{-4} was found. As a result, the film-diffusion stage might be regarded as the rate limiting phase for the whole process.

3.4 Effect of dye concentration and isotherm study

The study of adsorption isotherms describes the affinity, adsorbent's surface properties, and understanding of the equilibrium nature of the process (De Castro et al. 2018). Equilibrium dye adsorption on JLP was carried out using different dye concentrations and outcomes are depicted in Figure 11. In fact,

Table 6 Isotherm parametersfor AY 99 removal by JLP biomass

Langmuir isotherm				Freundlich isotherm			
q_{max}	K_L	R^2	χ^2	K_F	n	R^2	$\chi 2$
449.01	1.74×10^{-3}	0.983	264.61	10.89	2.036	0.932	502.64

the higher the dye concentration, the greater the driving force for mass transfer, thereby increasing the adsorption of dye before reaching equilibrium as proposed by Majumder et al. (2017). This phenomenon was well reflected in this experiment, according to which the maximum adsorption of AY-99 on JLP was found to be 418.15 mg g^{-1}at equilibrium, which was remarkably higher in comparison with previous research reports (Ozcan and Ozcan 2008; Khan et al. 2011;).

The isotherm study provides further mechanistic insights into the dye removal process by fitting the experimental outcomes to widely applied Langmuir isotherm (LI) and Freundlich isotherm (FI) equation. The Langmuir isotherm illustrates the conception of monolayer adsorption along with the homogeneous allocation of surface active sites on adsorbent. In contrast, the Freundlich model highlights multilayer heterogeneous adsorption behaviour (Naskar et al. 2016). The equations of Langmuir (Eq. 7) and Freundlich (Eq. 8) model are as follows (Khan et al. 2019; Naskar and Majumder 2017):

$$q_e = \frac{q_{max} K_L C_e}{1 + K_L C_e} \quad (7)$$

$$q_e = K_F C_e^{1/n} \quad (8)$$

Where q_e and q_{max} are the equilibrium and maximum dye adsorption (mg/g), respectively, C_e stands for dye concentration at equilibrium (mg L^{-1}), Langmuir affinity constant is represented by K_L (L mg^{-1}), K_F is Freundlich equilibrium constant reflecting of dye uptake capacity and n determines intensity of the adsorption.

The derived values of LI and FI model constants are shown in Table 6. Because of the higher correlation coefficient (0.983) and lower Chi-square value (264.61), the isotherm data make a reasonably good fit for the Langmuir model as compared to the Freundlich model (Majumder et al. 2017; Priyantha et al. 2018). Additionally, the empirical relationship between the theoretical adsorption capability deduced from the Langmuir isotherm (449.01 mg g^{-1}) and the experimentally measured value demonstrates the proximity (418.15 mg g^{-1}).

4 Conclusions

The most effective biomass for AY 99 adsorption from its aqueous phase is determined to be JLP biomass. The adsorption process, as demonstrated by UV-visible spectroscopic analysis, is highly influenced by the pH of the solution, which is optimum at 2.5. The outcomes of the experiments were very close to the predicted responses (R^2= 0.9915), according to optimal physicochemical parameters calculated via response surface methodology (RSM). Two independent variables (A and C) and two quadratic model terms (A^2 and C^2) are found to be the significant factors. The LI, PSO model, and film diffusion, all fit the equilibrium adsorption data well, implying that the dye molecules may adsorb physically and chemically on the biomass surface. Hence, JLP has a strong ability to decontaminate AY 99 dye from its aqueous phase, indicating its real application potential. Chemical modification and/or processing of the JLP biomass to activate or enhance the number of sorption sites could boost the extent of AY 99 elimination even more.

Abbreviations

CCD: Central Composite Design; RSM: Response Surface Methodology; ANOVA: Analysis of Variance; SOPE: Second-order polynomial model equation; SCT: Surface contact time; PFO: Pseudo first order; PSO: Pseudo second order; IPD: Intra particle diffusion; LI: Langmuir isotherm; FI: Freundlich isotherm; FOK: First order kinetic; SOK: Second order kinetic

References

Bagheri, R., Ghaedi, M., Asfaram, A., Dil, E. A., & Javadian, H. (2019). RSM-CCD design of malachite green adsorption onto activated carbon with multimodal pore size distribution prepared from *Amygdalusscoparia*: Kinetic and isotherm studies. *Polyhedron*, *171*, 464-472.

Basu, M., Guha, A. K., & Ray, L. (2017). Adsorption behavior of cadmium on husk of lentil. *Process Safety and Environmental Protection*, *106*, 11-22.

Cheruiyot, G. K., Wanyonyi, W. C., Kiplimo, J. J., & Maina, E. N. (2019). Adsorption of toxic crystal violet dye using coffee husks: equilibrium, kinetics and thermodynamics study. *Scientific African*, *5*, e00116.

Das, M., & Mishra, C. (2019). Jackfruit leaf as an adsorbent of malachite green: recovery and reuse of the dye. *SN Applied Sciences*, *1* (5), 1-8.

De Castro, M. L. F. A., Abad, M. L. B., Sumalinog, D. A. G., Abarca, R. R. M., Paoprasert, P., & de Luna, M. D. G. (2018). Adsorption of methylene blue dye and Cu (II) ions on EDTA-modified bentonite: isotherm, kinetic and thermodynamic studies. *Sustainable Environment Research*, *28*(5), 197-205.

Duque-Acevedo, M., Belmonte-Urena, L. J., Cortés-García, F. J., & Camacho-Ferre, F. (2020). Agricultural waste: Review of the evolution, approaches and perspectives on alternative uses. *Global Ecology and Conservation*, *22*, e00902.

Gupta, N. K., Gupta, A., Ramteke, P., Sahoo, H., & Sengupta, A. (2019). Biosorption-a green method for the preconcentration of rare earth elements (REEs) from waste solutions: A review. *Journal of Molecular Liquids*, *274*, 148-164.

Khan, M. M. R., Ray, M., & Guha, A. K. (2011). Mechanistic studies on the binding of Acid Yellow 99 on coir pith. *Bioresource Technology*, *102*(3), 2394-2399.

Khan, M., Motiar, R., Sahoo, B., Mukherjee, A. K., & Naskar, A. (2019). Biosorption of acid yellow-99 using mango (Mangiferaindica) leaf powder, an economic agricultural waste. *SN Applied Sciences*, *1*(11), 1-15.

Lellis, B., Fávaro-Polonio, C. Z., Pamphile, J. A., & Polonio, J. C. (2019). Effects of textile dyes on health and the environment and bioremediation potential of living organisms. *Biotechnology Research and Innovation*, *3* (2), 275-290.

Majumder, R., Sheikh, L., Naskar, A., Mukherjee, M., &Tripathy, S. (2017). Depletion of Cr (VI) from aqueous solution by heat dried biomass of a newly isolated fungus *Arthrinium malaysianum*: a mechanistic approach. *Scientific Reports*, *7*(1), 1-15.

Naskar, A., & Bera, D. (2018). Mechanistic exploration of Ni (II) removal by immobilized bacterial biomass and interactive influence of coexisting surfactants. *Environmental Progress & Sustainable Energy*, *37*(1), 342-354.

Naskar, A., & Majumder, R. (2017). Understanding the adsorption behaviour of acid yellow 99 on *Aspergillus niger* biomass. *Journal of Molecular Liquids*, *242*, 892-899.

Naskar, A., Guha, A. K., Mukherjee, M., & Ray, L. (2016). Adsorption of nickel onto *Bacillus cereus* M116: a mechanistic approach. *Separation Science and Technology*, *51*(3), 427-438.

Naskar, A., Majumder, R., & Goswami, M. (2020). Bioaccumulation of Ni (II) on growing cells of Bacillus sp.: response surface modeling and mechanistic insight. *Environmental Technology & Innovation*, *20*, 101057.

Ojha, A. K., & Bulasara, V. K. (2015). Adsorption characteristics of jackfruit leaf powder for the removal of Amido black 10B dye. *Environmental Progress & Sustainable Energy*, *34*(2), 461-470.

Ozcan, A. S., & Ozcan, A. (2008). Adsorption of Acid Yellow 99 onto DEDMA-sepiolite from aqueous solutions. *International Journal of Environment and Pollution*, *34*(1-4), 308-324.

Priyantha, N., Lim, L. B., Tennakoon, D. T. B., Liaw, E. T., Hei, C., & Liyandeniya, A. B. (2018). Biosorption of cationic dyes on breadfruit (*Artocarpus altilis*) peel and core. *Applied Water Science*, *8*(1), 1-11.

Putri, K. N. A., Kaewpichai, S., Keereerak, A., & Chinpa, W. (2021). Facile Green Preparation of Lignocellulosic Biosorbent from Lemongrass Leaf for Cationic Dye Adsorption. *Journal of Polymers and the Environment*, *29*(6), 1681-1693.

Ranasinghe, S. H., Navaratne, A. N., & Priyantha, N. (2018). Enhancement of adsorption characteristics of Cr (III) and Ni (II) by surface modification of jackfruit peel biosorbent. *Journal of Environmental Chemical Engineering*, *6*(5), 5670-5682.

Saha, P. D., Chakraborty, S., & Chowdhury, S. (2012). Batch and continuous (fixed-bed column) biosorption of crystal violet by Artocarpusheterophyllus (jackfruit) leaf powder. *Colloids and Surfaces B: Biointerfaces*, *92*, 262-270.

Saxena, M., Sharma, N., & Saxena, R. (2020). Highly efficient and rapid removal of a toxic dye: Adsorption kinetics, isotherm, and mechanism studies on functionalized multi-walled carbon nanotubes. *Surfaces and Interfaces*, *21*, 100639.

Uddin, M. T., Rukanuzzaman, M., Khan, M. M. R., & Islam, M. A. (2009). Adsorption of methylene blue from aqueous solution by jackfruit (Artocarpusheteropyllus) leaf powder: a fixed-bed column study. *Journal of Environmental Management*, *90*(11), 3443-3450.

Wang, Y., Wei, H., Wang, Y., Peng, C., & Dai, J. (2021). Chinese industrial water pollution and the prevention trends: An assessment based on environmental complaint reporting system (ECRS). *Alexandria Engineering Journal*, *60*(6), 5803-5812.